Int. J. of Thermodynamics
Vol. 9 (No. 4), pp. 1-11, December 2006
ISSN 1301-9724

Development of a Novel Modular Simulation Tool for the Exergy Analysis of a Scramjet Engine at Cruise Condition

Valentina Amati*, Claudio Bruno, Domenico Simone, Enrico Sciubba
Department of Mechanical & Aeronautical Engineering
University of Roma 1 "La Sapienza"
Via Eudossiana 18, 00184, Roma – Italy

Abstract

The scope of this work is twofold: first, to perfect the exergy approach to the design and optimization of aerospace propulsion systems; second, to develop a modular simulation tool in order to analyze potentialities and limits of different configurations of a scramjet engine. The vehicle is considered a "flying control volume" and is treated as a Large Complex Energy System ("LCES") to which systems balances (mass, energy, exergy) are applied to calculate the relevant losses for each one of its elementary devices. An energy and exergy analysis of a hydrogen-fueled scramjet is presented and discussed as a first application of the procedure that shall be extended to the analysis of different scramjet-configurations, fueled by H_2-alternative fuels: an exergy-based performance comparison can consequently complement an energy and thrust-based analysis.

All calculations have been performed with CAMEL®, an "in-house" modular process simulator code for energy conversion processes.

Keywords: scramjet, large complex energy system, exergy analysis.

1.Introduction

1.1 General description of a scramjet

A scramjet (acronym for Supersonic Combustion Ramjet) is a hypersonic airbreathing propulsion system, resulting from an evolution of the concept of a ramjet engine.

The basic principle of a ramjet is the same as that in a jet engine: intake, compression, combustion, and exhaust are the main operating stages. The incoming air flow is compressed by means of the so-called "ram compression effect"; the engine has no moving parts, the supersonic flow entering the intake is slowed to subsonic velocities (comparable to those reached in a turbojet) by aerodynamic diffusion created by properly shaped inlet and diffuser. The expansion of the hot gas, after the fuel injection and combustion, accelerates the exhaust air to a velocity higher than that at the inlet, producing positive thrust (see *Figure 1*). The speed of the vehicle must be high enough to compress the inlet air, in order to eliminate the need for turbocompressors.

A scramjet differs from a ramjet in that combustion takes place in a supersonic air stream (see *Figure 2*); compression at the intake is due to a system of oblique shock waves.

A scramjet engine can operate only at hypersonic speed (Mach numbers from 6 to about 24); thus scramjet-propelled vehicles must be accelerated to supersonic velocitiy by other means: recent tests of prototypes (NASA, 2004) used a booster rocket.

Scramjet potentiality and operability have been intensively studied in recent years because of the industrial interest in building aircraft that could fly "further and faster than a rocket" while maintaining their airbreathing characteristic (i.e. the possibility of using the external air as oxidizer, as opposed to carry additional oxygen and thus reaching a higher specific impulse).

In practice, vastly more complex problems are still awaiting a satisfactory solution in spite of the mechanically simple appearance of a scramjet: boundary layer/shock wave interaction modeling, turbulent mixing, two-phase flow, flow separation, combustion with very-fast

*Author to whom correspondence should be addressed

reacting species, real-gas aerothermodynamics and material stress are topics of active fundamental research, and demand both serious modeling efforts and large computing resources.

The high cost of flight testing and the unavailability of ground facilities have limited scramjets development to military applications: much of the current research funding comes from governmental defense research contracts. Some of the countries engaged in this effort are the USA, France, Russia and Australia (NASA, 2004; Schneider, 2002; SpaceDaily, 2001; Univ. of Queensland-HyShot, 2002).

A relatively near and promising commercial application could be that of using a scramjet as the first stage of a two-stage-to-orbit (reusable) launch vehicle. It must be remarked though that the possibility of employing scramjets as propulsion systems for commercial-manned vehicles is not feasible in the near term.

For more detailed and specific information on hypersonic propulsion systems, readers are referred to specific bibliographic references, like (Anderson, 2005; Brewer, 2000; Curran et al., 2000; Hayser et al., 1994).

1.2 Scramjet fuels

At present, hydrogen appears the most suitable fuel for a scramjet, for its high heating value, the complete absence of carbon (which avoids the problem of "coking" and of soot formation in the reactor; Kurabelnikov et al., 2003) and its high cooling capacity: liquid H_2 can be vaporized and pre-heated by means of a very effective heat recovery achieved by cooling the most thermally stressed surfaces of the vehicle.

But in spite of the very promising values of the computed specific thrust and impulse (on a mass basis, see TABLE I), difficulties and costs related with H_2 synthesis, transport and cryogenic storage (required by its low density, see TABLE II) press designers to search for different fueling solutions. Hydrocarbons have therefore been proposed as alternative fuels; among them, methane, which has a relative high density and the lowest carbon content, and some typical jet propellants (like kerosene); in either case the fuel would be reformed and the resulting syngas burned; the endothermic reforming reactions would be fed by the heat recovered in the burner cooling system. This would improve the quality of the pristine fuel (converting it into an "easier to burn" gas) and would increase its cooling capacity (Bruno et al., 2002).

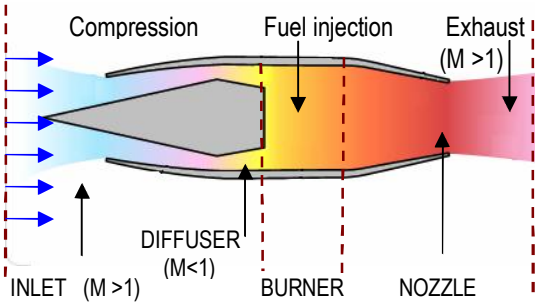

Figure 1. Schematic diagram of a ramjet engine.

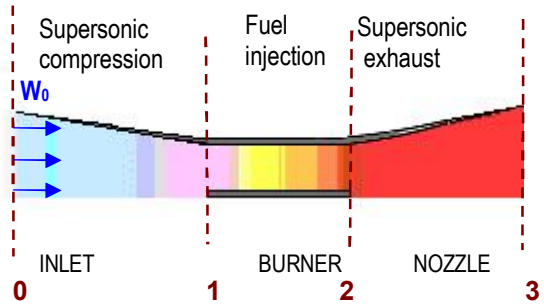

Figure 2. Schematic diagram of a scramjet engine.

TABLE I. MAIN PERFORMANCE PARAMETERS.

$$T_{sp}=F_T/m_0 = [(m_3W_3-m_0W_0)+10^{-3}(p_3-p_0)A_3]/m_0 \quad (1)$$

$$I_{sp}=F_T/(gm_f) = T_{sp}/gf \quad [g = 9.81\ m/s^2] \quad (2)$$

$$\eta_0 = (F_T W_0)/(10^3 E_{fuel}) \quad (3)$$

TABLE II. FUEL PROPERTIES.

	LHV		density
	[MJ/kg]	[MJ/m^3]	[kg/m^3]
H_2 (g), NC	120	10.8	0.0887
CH_4(g), NC	50	35.49	0.707
H_2 (l), 20 K	120	8.520	71
Kerosene (l), 293K	43	3.44 10^4	800

1.3 State of the art of the exergy analysis of propulsion systems. Purpose of the present work.

To determine the proper fueling method different aspects have to be considered: the physical and chemical properties of the fuel (density, LHV, specific heat, synthesis method); their influence on specific thrust and impulse; effective technical reliability (addressing the problems of combustion, thermal stress, need for auxiliary components, size and drag). The final purpose is to assess the "optimal" configuration and fuel both energetically (to reduce fuel consumption and increase efficiency) and in a more practical engineering sense (to guarantee the requested level of performance, durability and economics).

To this purpose, we decided to apply here to the field of aircraft propulsion the same principles and methodologies currently used in the analysis of ground-based energy conversion systems, and to use an exergetic approach.

Exergy analysis of aircraft engines is not new, and several applications have been published. We mention here Brilliant (1995); Horlock (1999) and Riggins et al. (2003), who addressed the need of introducing the concepts of "availability" and "second law efficiency" to propulsion systems; Rosen et al., who discussed the importance of defining a reference environment that varies with altitude (1999, 2000) and presented a first application on a turbojet engine (2004); Paulus et al., who proposed methods for accounting for the exergy rate associated with thrust and lift forces and for applying exergy flow diagrams to aircraft (2003); Bejan et al., who dealt with the optimization of the flying velocity and of the heat exchange processes on board (2001); Moorhouse et al., who introduced exergy methods for analyzing inlet performance (2002). Rancruel et al., (2003) investigated methods of optimization of the engine configuration; recently Bottini et al. (2003) first used the exergy method to assess the effect of an on-board fuel reforming on a scramjet. Many of these authors underlined the need of a further refinement of their methods.

The present work introduces in a more systematic way the method of exergy analysis to propulsion systems, and does this by capitalizing on the results of the previous contributions, perfecting and developing, when necessary, some aspects of the procedures. In the "system approach" we decided to adopt, the analysis is performed on a scramjet engine as a whole (and not on its individual components); the vehicle is considered a "Large Complex Energy System", and our goal is that of exploring the possibility of modifying the engine structure (i.e., configuration) to improve the overall mission performance.

The implementation of a specific utility in an existing process simulator has been a necessary stage of the work.

We present here a first, simple but basically complete, application to an H_2-fueled scramjet.

The modeling procedure will be described in detail; the results of the calculations will be compared to available literature data which include both experimental and theoretical results (Heyser et al, 1994; Curran et al., 2000); finally, the influence of some key assumptions on the results of the analysis are briefly discussed as well.

2. The Simulation Code

The novel modular model of the scramjet has been implemented and integrated in an existing process simulator, CAMEL® (Fiorini et al., 2005 a-b). This code is written in C++ language, is based on a completely and genuine object-oriented approach, and is equipped with a user-friendly graphical interface that allows for the simulation and analysis of several energy conversion processes (thermal power plants and desalination plants). The system is represented as a network of components connected by material and energy streams; each component is characterized by a set of equations describing the thermodynamic changes imposed on the streams; in mathematical terms, this equation system is not a closed one, and it therefore needs a sufficient number of proper boundary conditions in terms of known flow parameters. In practical terms, this means that this equation system depends on both the plant configuration and the assigned boundary conditions. An optimized iterative Newton-Raphson algorithm is used to solve the global equation system.

The main feature of CAMEL® is in effect its modularity that allows users to expand the code by adding new components or by improving the model of the existing ones; we exploited these capabilities to introduce the proper process equations for the scramjet model.

3. Scramjet Modeling

3.1 The thermodynamic cycle and the representative components

The basic configuration of the scramjet has been decomposed into the following elementary components, each embodying a specific process:

1. Inlet, compression process;
2. Burner, combustion process;
3. Nozzle, expansion process.

The method is thus based on a classical "black-box" approach; each component has been analyzed considering the thermodynamic transformations it imposes on the fluid flowing through it; where necessary, the component operating parameters have been computed "externally" with a non-lumped procedure.

The open-Brayton cycle has been studied by evaluating the thermodynamic state of the air and of the combustion products in each representative point on the (s, h) diagram and by applying the fundamental conservation equations (mass, energy and momentum) to a specified control volume. The code provides quantitative information about all the main variables (m, p, T, h, ex, W, s) and in a post-processing step it

evaluates the propulsive performances (T_{sp}, I_{sp}, η_0) and performs an exergy analysis.

3.2 General assumptions

The following assumptions have been made:

a. The flying control volume consists solely of the engine in which the thermodynamic cycle is realized; all the interactions with the rest of the vehicle (i.e. heat transfer with the external surfaces of the vehicle, external drag of the lifting body) are not included; all control and regulating systems are neglected.

b. The system as a whole is assumed to be at steady state, flying at cruise condition. The one-dimensional treatment proposed in (Heyser et al., 1994) was adopted.

c. Air and exhaust gases are considered thermally perfect (TPG), following the law $p/\rho = ZRT$ with the compressibility factor Z is taken equal to 1; since this implies $p_R<2$ and $T_R>1.8$, it follows that the minimal cycle temperature must be 230K and the maximum pressure 75atm. Both values fall well within the limits of the present simulation. The gas thermodynamic properties (c_p and enthalpy) are calculated by the code with an analytical formulation that provides values very close to the experimental data of the JANAF tables (in the assumption of a TPG, see Lanzafame et al., 2000; Lienhard, 1981).

d. The chemical equilibrium composition is calculated for the combustion products (ideal reactor with infinite residence time); dissociation phenomena are neglected.

e. All working media flowing in and out of each component are assumed to have uniform properties (they are devoid of local gradients).

3.3 Component models

In this paragraph the main equations and relationships used in the calculation are presented and briefly discussed; additional details are reported in the Appendix.

3.3.1Inlet and nozzle

The air conditions at station 0 are the free stream air conditions. The following equations are used:

Mass flow rate conservation:

$$m_{out} = m_{in} \quad (4)$$

Conservation of energy (total enthalpy):

$$h_{t,in}(1-\sigma) = h_{t,out} \quad (5)$$

with

$$h_t = ½10^{-3}W^2 + h \quad (6)$$

s is a loss coefficient (Heyser et al., 1994) that takes into account the total enthalpy losses due to the heat transfer from the air (gas) stream to the boundary of the control volume.

Equations for the adiabatic, non-isentropic transformation:

$$\beta = p_{out}/p_{in} = (T_{out,i}/T_{in})^{Cp/R} \quad (7)$$

$$\eta_{inl} = (h_{1i}-h_o)/(h_1-h_o) \quad (8)$$

$$\eta_{noz} = (h_2-h_3)/(h_2-h_{3,i}) \quad (9)$$

with $\beta = p_1/p_o$ (inlet) or $\beta = p_3/p_2$ (nozzle). In Equation (7) an average constant value of the c_p (between the inlet and the outlet temperature) is computed at each iteration of the solving algorithm.

The adiabatic efficiencies can either be assigned as constant (if they are known) or evaluated as functions of the flying conditions (Mach number). The performance of the inlet has been evaluated according to the analysis proposed in (Simone et al., 2005). The geometry of the inlet and the trend of η_{inl} and β are discussed in the Appendix. This coefficient (η_{inl}) accounts for the losses due to the oblique shock waves and to friction (internal friction of the flow and friction on the endwalls).

The performance of the nozzle has been evaluated according to the procedure reported in (Curran et al., 2000) and described in the Appendix.

3.3.2 Burner

The combustion process takes place at constant pressure. The most relevant (and questionable!) simplifications are made in the modeling of this component; it is assumed that the products are in chemical equilibrium. The following equations are used:

Conservation of mass:

$$m_1 + m_{fuel} = m_2 \quad (10)$$

Conservation of energy:

$$m_1(h_1 + ½10^{-3}W_1^2 + f\,10^{-3}W_f^2 + \eta_b\, f_c 10^3 LHV + +f\,h_f) = m_2\,(h_2 + ½10^{-3}W_2^2) + q \quad (11)$$

$$f_c = f \text{ if } f < f_{stoich} \text{ otherwise } f_c = f_{stoich}$$

where η_b is the combustion energy efficiency and q is the thermal power exchanged by the burner (because of heat losses or heat removal for cooling); if the reactor is adiabatic q is set equal to zero.

Conservation of momentum (with $p_1=p_2$):

$$W_1 + f\,W_{fx} - \tfrac{1}{2}C_f(A_w/A_1)W_1 = (1+f)W_2 \quad (12)$$

W_{fx} is the injection velocity of the fuel in the axial direction and $\frac{1}{2}C_f(A_w/A_1)$ is the drag coefficient of the burner (Heyser et al., 1994).

4. Exergy Analysis Applied to Propulsion Systems

4.1 Exergy definition

Considering a control volume analysis, the exergy rate of a stream of matter m is computed on the basis of its physical, potential, kinetic and chemical terms (Equations 13-17); the contributions of other energy forms (magnetic, nuclear) have been neglected.

$$Ex = m\,(ex^{PH} + ex^{P} + ex^{K} + ex^{CH}) \quad (13)$$

$$ex^{PH} = (h-h_0) - T_0(s-s_0) \quad \text{(physical)} \quad (14)$$

$$ex^{CH} = RT_0 \sum_i y_i \ln (y_i/y_{i,0}) \quad \text{(chemical)} \quad (15)$$

$$ex^{P} = g(z-z_0)\,10^{-3} \quad \text{(potential)} \quad (16)$$

$$ex^{K} = \tfrac{1}{2}\,10^{-3}C^2 \quad \text{(kinetic)} \quad (17)$$

y_i and $y_{i,0}$ denote respectively the molar fraction of the i^{th} species of the gas at the state defined by (p, T) and in the reference environment (see paragraph 0). Fuel exergy has been also evaluated accounting for all the above listed four contributions; since "fuel" of course does not exist as such in the reference environment, its chemical exergy has been calculated considering an ideal combustion reaction involving reference substances (Baehr 1973; Baehr et al., 1963)

The exergy rates associated with power (thrust work) or heat interaction have been evaluated according to the following expressions:

$$Ex_T = F_T\,W_0\,10^{-3} \quad (18)$$

$$Ex_q = q\,(1 - T_0/T_{bn}) \quad (19)$$

where T_{bn} is the boundary temperature at which heat is exchanged.

A complete description of the methods and principles of exergy analysis can be found in (Bejan et al., 1996; Moran et al., 1994; Kotas, 1985; Szargut et al., 1988)

4.2 Reference environment

The reference environment is the unperturbed free stream air at the flying altitude: p_0 and T_0 are equal to the external air pressure and temperature. Considering that the simulations have been performed for different cruise speeds (M_0 = 6÷14) and imposing a constant dynamic pressure trajectory, it follows that the air conditions and the flying altitude change with the flight speed. The correspondent air static pressure is valuable considering Equations -:

$$p_{dyn} = 0.5\,\rho_0 V_0^2\,10^{-3} \quad \text{(dynamic pressure)} \quad (20)$$

$$V_0 = a_0 M_0 = (10^3\,k_0 RT_0)^{1/2}\,M_0 \quad (21)$$

$$\rho_0 = p_0 / (RT_0) \quad \text{(perfect gas law)} \quad (22)$$

$$p_{dyn} = 0.5\,p_0\,k_0 M_0^2 \;\Rightarrow\; p_0 = 2p_{dyn}/(k_0 M_0^2) \quad (23)$$

In a first-order approximation, air composition is assumed constant with altitude and equal to the main composition of the U.S. Standard Atmospheric Air (21% of O_2 and 79% of N_2 on a molar basis).

The air absolute velocity C_0 (wind velocity) is assumed equal to zero; thus, the relative velocity of the air in respect to the vehicle, W_0, is equal and opposite to the absolute cruise speed of the scramjet; the kinetic exergy can consequently be calculated as $ex^K = \frac{1}{2}10^{-3}(C)^2 = \frac{1}{2}10^{-3}(W-W_0)^2$.

4.3 Process analysis: exergy accounting

A scheme of the system structure is presented in *Figure 3*: the arrows indicate the matter and energy exchanges between components with the associated exergy rates.

Mass and energy balances were computed along the lines of the "stream thrust analysis" (Heyser et al., 1994) as reported in section 0. Therefore, the laws of conservation can be written (for a control volume at steady state) in this "balance" form:

$$\text{Mass:} \quad \sum m_{in} - \sum m_{out} = 0 \quad (24)$$

$$\text{Energy:} \quad \sum E_{in} - \sum E_{out} = 0 \quad (25)$$

Exergy accounting consists in the combined application of the First and Second Laws to a thermodynamic system. Consequently, the exergy flow "accounting" necessarily contains a term representative of the losses within the component (exergy destruction, Ex_d):

$$\text{Exergy:} \quad \sum Ex_{in} - \sum Ex_{out} = Ex_d \quad (26)$$

The terms E_{in},E_{out}, Ex_{in} and Ex_{out} contain all the energy and exergy rates associated with mass flows and with work and heat interactions.

The purpose of an exergy analysis is that of detecting and calculating these irreversible losses, and consequently apply the proper methodologies in order to minimize them. Notice that this is also the scope of energy ("first law") analysis: only, there is an obvious difference in minimizing the exergy, rather than the energy losses: of all the streams that are discharged into the environment and whose *energy* content constitutes a "loss" for the system, not all have a high *exergy* content, and therefore the real loss (intended as the missed opportunity to extract further useful work from the system) may take different values. In contrast, there may be some of the losses that are practically *unavoidable* from an entropic point of view (e.g.: combustion

and heat exchange processes), and also in such cases an energy analysis does not reflect, in this sense, the proper physics of the process.

Figure 3 shows also the "uninstalled" thrust force F_T resulting from the contribution of each component and decreased of their internal drag. This force must be equal to or higher than the external drag of the vehicle if the scramjet has to effectively realize, respectively, a cruising or an accelerating mission; moreover, the necessary lifting force must be produced to sustain the aircraft or make it climb. The solution of both these design constrains is outside the scope of the present work and shall not be discussed here.

Further work is in progress to enlarge the boundaries of the control volume, by sizing and including the rest of the vehicle: with additional information on dimension, geometry and weight of the scramjet it would be possible to estimate the external drag, the net thrust force (or "installed thrust") and the lift force, allocating them among the devices (engine, tanks, auxiliary components, structures, wings or lifting surfaces) (Gaggioli et al., 2003).

4.4 Exergy-based performance parameters

The exergy efficiency of a system is defined as the ratio between the exergy of the useful output and the exergy resource influx to the system (fuel total exergy).

Thus for a scramjet, where thrust power is the useful output, we have:

$$\varepsilon = Ex_{,T}/Ex_{,f} \quad (27)$$

and for the individual components:

$$\text{Inlet:} \quad \varepsilon_{inl} = Ex_1/Ex_{T,inl} \quad (Ex_0 = 0) \quad (28)$$

$$\text{Burner:} \quad \varepsilon_b = Ex_2/(Ex_1+Ex_f+Ex_{T,b}) \quad (29)$$

$$\text{Nozzle:} \quad \varepsilon_{noz} = Ex_{T,noz}/Ex_2 \quad (30)$$

where the useful outlet exergy of the nozzle is equal to $Ex_{T,noz}$ while the term Ex_3 is the exergy rate discharged into the environment with no further recovery.

To assess the engine performance and to identify the most critical processes, the following parameters can be evaluated to show what percentage of the total exergy resource is destroyed within each component:

$$\delta_1 = Ex_{dj}/Ex_{d,tot} \times 100\% \quad (31)$$

$$\delta_2 = Ex_{dj}/Ex_{fuel} \times 100\% \quad (32)$$

δ_1 is the ratio, expressed in %, of the exergy destroyed in the j^{th} component to the total exergy destroyed in the system.

δ_2 is the percentage of the total exergy resource influx into the process that is destroyed in the j^{th} component.

5. Analysis of a H_2-Fueled Scramjet

5.1 Flying conditions

Simulations have been performed for flight Mach numbers M_0=6÷14 and for a constant dynamic pressure trajectory equal to 86.18 kPa (1800 psf).

The external air static pressure and the corresponding temperature, density and altitude are reported in TABLE III of the Appendix.

5.2 Simulations

Simulations have been run according to the procedure reported in section 3; three different sets of assumptions have been imposed in order to show "how" and "how much" some simplifications usually adopted can influence the results; in the following they will be indicated as cases 1, 2 and 3:

Case 1:

- Component efficiencies vary with Mach;
- The drag of the burner and the fuel momentum are included in the equations. The drag coefficient is set equal to 0.02 (Heyser et al., 1994).

Case 2:

- Component efficiencies vary with Mach;
- The drag of the burner and fuel momentum are neglected (consequently W_3=W_2).

Case 3:

- Component efficiencies are constant and equal to their maximum value.
- The drag of the burner and fuel momentum are neglected.

For all cases an adiabatic burner is assumed and the fuel is injected at 500 K with negligible relative velocity; an adapted nozzle configuration has been assumed ($p_3 = p_0$).

All figures refer to the case of an equivalence ratio Φ=1.

, 5, 6 report the trends of the specific impulse, of the specific thrust and of the overall efficiency. Their dependence on the Mach number is in line with the data reported by (Curran et al., 2000; Heyser et al., 1994).

5.3 Results

It is apparent how the neglection of the variation in the operating conditions (assuming

constant efficiencies, case 3) and of the internal drag affects the results. For low Mach numbers differences between cases 2 and 3 in respect to case 1 (assumed as "base case") are limited to 3-5% (for all three parameters: I_{SP}, T_{sp} and η_o), but they increase to 30% above Mach 12: the assumption of constant efficiencies can strongly influence the results and this simplification must be clearly justified (constant efficiency can be reasonable, in a restricted range of flying condition, only if we adopt an inlet with variable geometry).

-9 show the results of the exergy analysis (for case 1); the overall and the exergetic efficiency () assume almost the same value; they express the ratio between thrust power and, respectively, fuel energy and exergy, which have similar values.

The maximum reached at Mach 12 was expected, since in this example the inlet geometry was designed in order to attain the best "overall" performance (net thrust power) exactly at this cruise velocity. The maximum of ε is reached for an M_0 near to 10 because of the higher increase of the fuel exergy with Mach with respect to its energy: while fuel enthalpy is constant (constant injection temperature), its physical exergy increases because of the changing reference environment.

The total exergy destruction increases with Mach (), and its main fraction is due to the burner (), as expected. All components present values of the entropy generation rates that increase with Mach; both inlet and nozzle display a decreasing adiabatic efficiency, which is representative, under the adopted "lumped" approach, of the increasing internal friction of the flow and of the losses due to shock waves. Also, the drag of the burner increases quadratically with the inlet velocity and the combustion energy efficiency (which takes into account the incomplete degree of reaction due to the decreasing residence time in the burner) decreases.

5.3.1 Exergy analysis: component performance

- Inlet: all performance parameters ($Ex_{d,inl}$, ε_{inl}, $\delta_{1,inl}$, $\delta_{2,inl}$) consistently reflect the increasing irreversibility within this component, both in absolute terms ($Ex_{d,inl}$, ε_{inl}) and with respect to the other components ($\delta_{1,inl}$, $\delta_{2,inl}$): the percentage of the total exergy destruction remains much lower than that of the burner, but for M_0 >9 it results $\delta_{1,inl} > \delta_{1,noz}$. It is important to underline that this result depends essentially on the preliminary assumption made on the variation of the component performance with the flight conditions (see Appendix).

- Nozzle: in this case, despite the increasing total exergy destruction of the component (and the consequent decreasing of the ratio Ex_{out}/Ex_{in}), the exergy cumulatively discharged into the environment (Ex_3) decreases, thus generating a higher thrust power transmitted to the vehicle. The "thrust efficiency" Ex_T/Ex_{in} of the nozzle increases and reaches a maximum near Mach 14, consistent with the trend of the total thrust power of the engine (which is negatively affected by the drag of the inlet and of the burner).
- Burner: although this component is the main source of irreversibility in the engine, we notice a slight improvement of its exergy efficiency with M_0: the total enthalpy of the incoming air (and consequently the associated exergy rate Ex_2) is an increasing fraction of the total energy input to the reactor. This "thermal" exergy of the air becomes predominant with respect to the chemical exergy brought by the fuel and irreversibly transformed in thermal exergy, thus reducing the incidence of this irreversible conversion on the final "output" of the burner (high-T flue gas). For comparison, the air inlet temperature rises from 550 K (M_0=6) to 1500K (M_0=14) and the inlet pressure increases from 0.65 to 1.3 bar.

6. Conclusions

The present study is preliminary, both in its system approach and in its thermodynamic formulation, and its main purpose is that of illustrating the specific application of the exergy method to a scramjet vehicle. In fact, although some simplifiying assumptions, the development of the procedure and its application are methodologically rigorous and illustrate in detail the specific application of the exergy analysis to a scramjet vehicle.

These preliminary results show though that the present approach is certainly worth pursuing: a simple H_2-fueled scramjet has been analyzed by means of a novel specific utility implemented in an existing process simulator, and the influence of some relevant assumptions on the results have been discussed: the simulation results respect trend and magnitude for what concern the calculated values of specific thrust and impulse.

The exergy analysis clearly identifies both losses and destruction in the various components, apportioning them among the different devices.

It is useful to recall that an exergy analysis does not only identify but also quantify the cause of each irreversible loss, and provides the designer with more physical insight into the phenomenological side of the process: in the "base-case" discussed here, the exergy flow diagrams confirm the predominant (negative) role of the burner on the overall performance and underline its high sensibility to the flow inlet conditions. Preheating and a higher inlet pressure reduce the irreversibility rate connected with the chemical reaction but at the same time negatively affect its conversion efficiency.

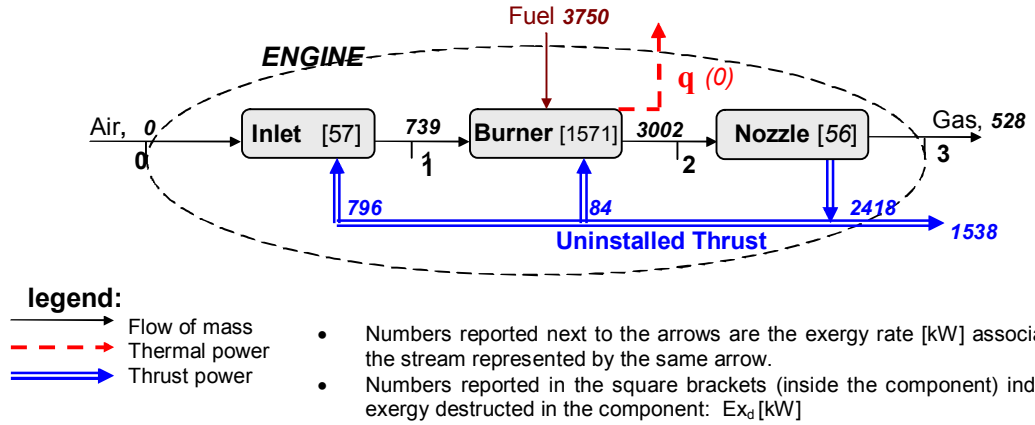

Figure 3. Engine control volume (data refer to case 1, Mach 10, F =1).

Legend of Figures , *5* ,*6*: numbers "1", "2", "3" refer respectively to Cases 1, 2, 3 (see paragraph 0)

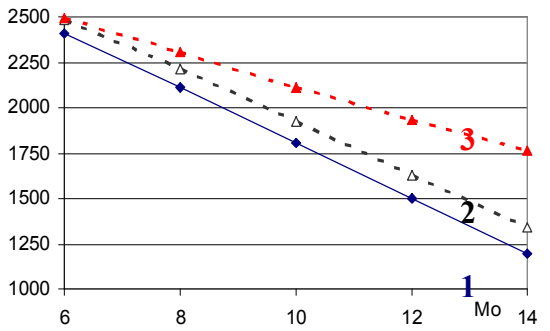

Figure 4. Specific impulse [s].

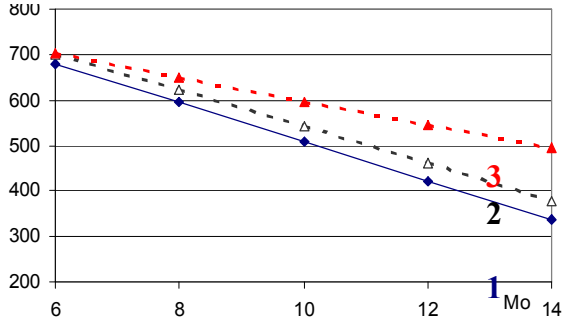

Figure 5. Specific thrust[m/s].

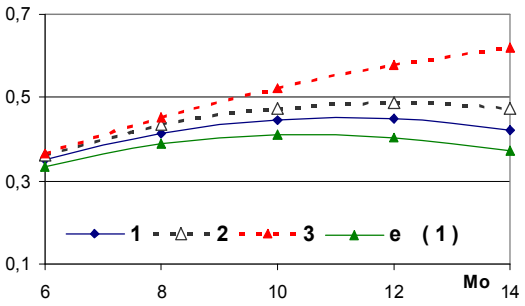

Figure 6. Overall (1,2,3) & Exergy efficiency (1).

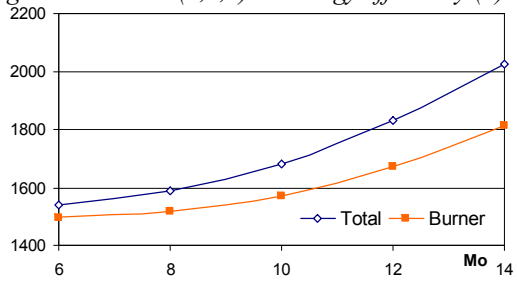

Figure 7. Total exergy destruction [kW].

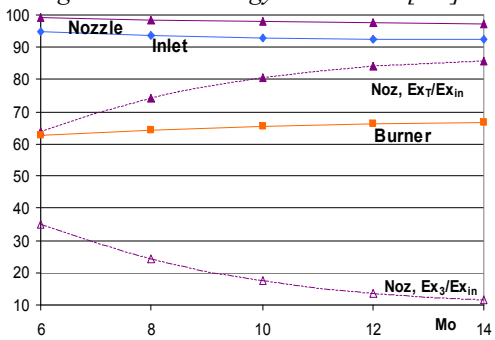

Figure 8. Components' exergy efficiency[%].

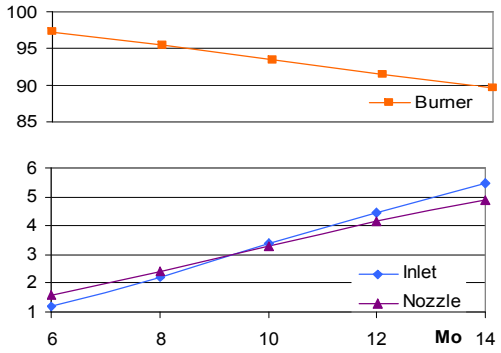

Figure 9. Components' exergy destruction, δ_1 [%].

List of Symbols

A	Cross area [m^2]
C	Absolute velocity [m/s]
c_p	Specific heat at constant pressure [kJ/kgK]
E	Energy rate [kW]
Ex	Exergy rate [kW]
Ex_d	Exergy deswtruction [kW]
ex	Specific exergy [kJ/kg]
f	Fuel/Air mass ratio (m_{fuel}/m_{air})
f_{stoich}	Fuel/Air stoichiometric mass ratio
F	Force [N]
h	Specific enthalpy [kJ/kg]
I_{sp}	Specific impulse [s]
LHC	Liquid hydrocarbon
LHV	Lower heating value [MJ/kg]
m	Mass flow rate [kg/s]
p	Pressure [kPa]
p_{dyn}	Dynamic pressure [kPa]
p_R	Reduced pressure [kPa]
q	Thermal power [kW]
R	Constant of gas [kJ/kgK]
s	Specific Entropy [kJ/kgK]
T_{sp}	Specific thrust [m/s]
T	Temperature [K]
T_R	Reduced temperature [K]
W	Relative velocity [m/s]
Φ	Equivalence ratio (f/f_{stoich})
$\delta_{1,2}$	Exergy destruction coefficients
ε	Exergy efficiency
η, η_o	Efficiency, Overall efficiency
σ	Loss coefficient

Suffixes:

b	Burner
inl	Inlet
noz	Nozzle
f	Fuel
i	Ideal
in	Inlet (entrance)
out	Outlet (exit)
t	Total
T	Thrust

References

Anderson, J. D., Jr, 2005, *Introduction to flight*, McGraw Hill International Edition, Singapore.

Baehr, H. D., 1979, The Exergy of Fuels, *BWK*, v. 31, n. 7, pp. 292-297 (in German).

Baehr, H. D., Schmidt, E. F., 1963, Definition and Calculation of the Exergy of Fuels, *BWK*, v. 15, n. 8, pp. 375-381 (in German).

Bejan, A., Siems, D. L., 2001, The Need for Exergy Analysis and Thermodynamic Optimization and Aircraft Development, *Exergy Int. J.*, Vol. 1 (No. 1), pp. 14-24.

Bejan, A., Tsatsaronis, G., Moran, M., 1996, *Thermal design and optimization*, J. Wiley.

Bottini, H., Bruno, C., Sciubba, E., 2003, Exergy Analysis of a Scramjet Operating at Cruise Conditions with an on-Board Fuel Reformer, presented at the *European workshop on exergy analysis for aerospace application*, Bourges, August 26-28.

Brewer, G. D., 2000, *Hydrogen aircraft technology*, CRC press, Boca Raton, Florida.

Brilliant, H. M., 1995, Analysis of Scramjet Engines Using Exergy Methods, *AIAA* 95-2767.

Bruno C., Filippi, M., 2002, Reforming and Pyrolisis of Liquid Hydrocarbons and Partially Oxidised Fuels for Hypersonic Propulsion, in: *Combustion and Energetic Materials*, Kuo, Kenneth K., De Luca, Luigi T. eds., Begell House, Inc., NY-Wallingford U.K.

Curran, E. T., Murthy S. N. B., 2000, Scramjet Propulsion, *Progress in astronautics and aeronautics*, Vol. 189, AIAA.

Fiorini, P., Sciubba, E., 2005 (a), A Novel Modular Simulation Code for Multi-Stage Flashing Desalination Plants, *ATC 2005 Conference*, Istanbul, Turkey, May 2005

Fiorini, P., Sciubba, E., 2005 (b), Modular simulation and Thermoeconomic Analysis of a Multi-Effect Distillation desalination plant, *Proc of ECOS 2005*, Trondheim, Norway, June 2005.

Hayser, W. H., Pratt, D. T., 1994, *Hypersonic Airbreathing Propulsion*, AIAA Education Series, Washington.

Horlock, J., 1999, Thermodynamic Availability and Propulsion, AIAA *ISABE 99*-741.

Kotas, T., 1985, *The exergy method of thermal plants analysis*, Butterworth.

Kurabelnikov, A. V., Kuranov, A. L., 2003, Low-Temperature Steam Reforming of Liquid Hydrocarbon Fuel, *41st Aerospace Sciences Meeting and Exhibit*, January, Reno, Nevada, AIAA 2003-1167.

Lanzafame, R., Messina M., 2000, A new Interpolating Polynomial for the Evaluation of

Gas Enthalpy (in Italian), *La Termotecnica*, n°11, November.

Lienhard, J. H., 1981, *A heat transfer textbook*, Prentice Hall, Inc., Englewood Cliffs, NJ.

Moorhouse, D. J., Hoke, C. M., 2002, Thermal Analysis of Hypersonic Inlet Flow with Exergy-Based Design Methods, *Int. J. Applied Thermodynamics*, Vol. 5, No. 4, pp. 161-168, December.

Moran, M. J., Sciubba, E., 1994, Exergy Analysis: Theory and Practice, *J. Eng. for GT and Power*, v. 116, April.

Paulus, D. M. Jr., Gaggioli, R. A., 2003, The Exergy of Lift, and Aircraft Exergy Flow Diagrams, *Int. J. Thermodynamics*, Vol. 6, No. 4 pp. 149-156, December.

Rancruel, D. F., Von Spakovsky, M. R., 2003, Decomposition with Thermoeconomic Isolation Applied to the Optimal Synthesis/Design of an Advanced Fighter Aircraft System, *Int. J. of Thermodynamics*, Vol. 6, No. 3.

Riggins, D., 2003, The Thermodynamic Continuum of Jet Engine Performance: The Principle of Lost Work due to Irreversibility in Aerospace System, *Int. J. Thermodynamics*, Vol. 6 (No. 3), pp.107-120, September.

Rosen, M. A., Etele, J., 1999, The Impact of Reference Enviromene Selection on the Exergy Efficiencies of Aerospace Engines, *Proc. of the ASME*, *Advanced Energy System Division*, Vol. 39, pp. 583-591, ASME.

Rosen, M. A., Etele, J., 2000, Sensitivity of Exergy Efficiencies of Aerospace Engines to Reference Enviroment Selection, *Int. J. Exergy*, Vol. 1, No. 2, pp. 91-99.

Rosen, M.A., Etele, J., 2004, Aerospace System and Exergy Analysis: Application and Methodology Development Needs, *Int. J. Exergy*, Vol. 1, No. 4, pp 411-425.

Simone, D., Bruno, C., 2005, Silanes as Fuel for SCRJ, *AIAA CIRA 13th International Space Planes and Hypersonic System and Technologies*, AIAA 2005-3398.

Szargut, J., Morris, D.H., Steward, F.R., 1988, *Exergy analysis of thermal, chemical, and metallurgical processes*, Springer-Verlag.

References on the web:

American Scientist, 2005, December

Available at: www.aiaa.org

NASA website for National Hypersonic Plan, 2004, Release 16.04: NASA's X-43A Scramjet Breaks Speed Record.

Available at: http://www.nasa.gov

Schneider, D., 2002, A Burning Question: When was the first scramjet flight-tested? American Scientist online.

Available at: http://americanscientist.com

SpaceDaily, 2001, Hypersonic Scramjet Projectile Flys in Missile Test.

Available at: http://www.spacedaily.com

University of Queensland Centre for Hypersonics- HyShot™

Available at: http://www.mech.uq.edu.au

Appendix

A 1 Inlet performance

Conditions at the entry of the burner were calculated in a previous work (Simone et al., 2005) for the selected Mach numbers, assuming that the flow is compressed by three shocks ahead of the cowl lip of a hypersonic inlet that coalesces onto the cowl lip at a Mach number just above 12. The geometry is shown in *Figure 10* while the conditions of the air after the shocks are reported in TABLE III.

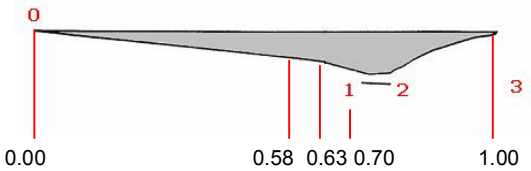

	ramp angle	rel x dist
ramp 1	4.0	0.58
ramp 2	8.0	0.63
ramp 3	13.0	0.70
throat	0.0	0.72

Figure 10. Schematic representation of the inlet geometry.

TABLE III. FLOW CONDITIONS UPSTREAM AND DOWNSTREAM THE SHOCK WAVES SYSTEM.

M_0	p_o [kPa]	T_0 [K]	W_0 [m/s]	p_1 [kPa]	T_1 [K]	W_1 [m/s]
6	3.424	220.3	1785.3	64.9941	549.4	1589.4
8	1.925	224.3	2401.5	74.9114	726.1	2181.5
10	1.236	226.9	3019.5	89.8328	937.1	2773.2
12	0.851	230.3	3650.5	108.34	1191.9	3375.5
14	0.628	235.3	4305.2	129.654	1501.0	3999.0

On the basis of this analysis it is possible to express the intake performance by means of two parameters: the adiabatic efficiency η_{inl} and the compression ratio β. Their trend with the Mach number is shown in *Figure 11*.

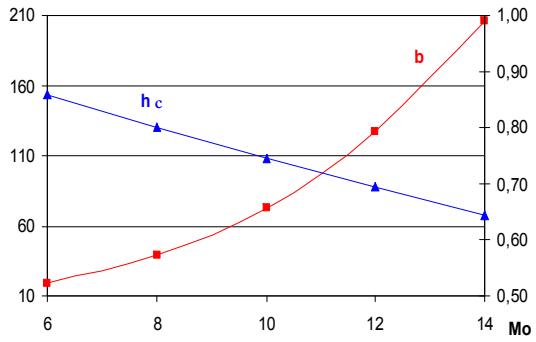

Figure 11. Inlet adiabatic efficiency and compression ratio.

A 2 Nozzle performance

The adiabatic efficiency η_{noz} is evaluated (according to Curran et al., 2000) as a function of the flying condition; the following expressions have been used:

$$\eta_{noz} = [C_{ev}^2 - (W_2/W_{3i})^2] / [1 - (W_2/W_{3i})^2] \quad (33)$$

$$C_{ev} = 0.98 \quad (34)$$

$$\eta_{kin} = (W_3/W_{3i})^2 \quad (35)$$